*Anal. Bioanal. Electrochem.*, Vol. 10, No. 9, 2018, 1134-1143

**Analytical & Bioanalytical Electrochemistry**

2018 by CEE
www.abechem.com

*Full Paper*

# A Simple Electrochemical Fabrication and Characterization of Superparamagnetic Composite of Nickel Doped Iron Oxide/Carbon Nanoparticles

**Kamal Yavari[1] and Behrouz Sabour[2,*]**

[1]*Materials and Nuclear Research School, Nuclear Science and Technology Research Institute (NSTRI), P.O. Box 14395-834, Tehran, Iran*
[2]*Department of Chemistry, Amirkabir University of Technology (Tehran Polytechnic), 15875-4413 Tehran, Iran*

*Corresponding Author, E-Mail: b.sabour@aut.ac.ir

*Received: 2 June 2018 / Received in revised form: 21 July 2018 / Accepted: 30 July 2018 / Published online: 30 September 2018*

**Abstract**- In this research, composite of metal ion doped $Fe_3O_4$ nanoparticles/carbon are prepared via cathodic electrochemical synthesis for the first time. The carbon dispersed aqueous solution of iron(III) nitrate, iron(II) chloride and nickel nitrate was used as the deposition electrolyte. The synthesis was done with applying 10 mA $cm^{-2}$ at RT conditions. The prepared composite were characterized through XRD, IR, SEM and VSM analyses. The particle morphology, carbon content and metal ion doping were verified by SEM observations and energy-dispersive X-ray spectroscopy. XRD and IR data confirmed that the fabricated composite has magnetite crystal structure. The magnetic data of *Ms*=54.83emu $g^{-1}$, *Mr*=0.43 emu $g^{-1}$ and *Hci*=9.26 G, obtained by VSM analysis, proved the superparamagnetic nature of the fabricated composite.

**Keywords-** Iron oxide, Metal-ion doping, Electrochemical synthesis, Nanocomposite

## 1. INTRODUCTION

Iron oxide ($Fe_3O_4$) nanoparticles (NPs) have been widely investigated for biomedical uses like as magnetic resonance imaging (MRI) contrast enhancement, cancer treatment using hyperthermia therapy and targeted drug delivery, as a results of their moderate cytotoxicity

profile, inherent magnetic property and high specific absorption rate [1]. However, it was reported that utilization of iron oxide NPs in both *in-vitro* and *in-vivo* applications encounter with distinct obstacles [2]. For instance, the bare pristine $Fe_3O_4$ NPs show tendency to agglomeration, where results the bigger particles formation with strong anisotropic dipolar interaction aqueous media [3]. Due to this, $Fe_3O_4$ NPs miss their colloidal stability and magnetic properties that ultimately reduce their performance. Furthermore, the agglomeration of $Fe_3O_4$ NPs often leads precipitation as they administered in-vivo, which results shortening of circulation time in the blood [4]. Hence, there is a necessity to coat $Fe_3O_4$ NPs surfaces and/or compositing with suitable agents to solve the problems related to the agglomeration and precipitation in aqueous suspension [5-9]. In this regards, polymer- and carbon- based composites of magnetite ($Fe_3O_4$) nanoparticles have been recently extensively studied [10-16]. For example, Zhang et al. [11] synthesized superparamagnetic iron oxide nanoparticles modified with polyethylenimine (PEI) and poly(ethylene glycol) methyl ether (MPEG) through a photochemistry method and investigated their performance as new MRI contrast agent. Chen et al. [12] report composites of Aminodextran-coated $Fe_3O_4$ nanoparticles and graphene oxide (GO) for cellular magnetic resonance imaging and their results indicated that compared with the isolated $Fe_3O_4$ NPs, the $Fe_3O_4$-GO composites showed significantly enhanced cellular MRI, being capable of detecting cells at the iron concentration of 5 μg $mL^{-1}$ with cell density of $2\times10^5$ cells $mL^{-1}$, and at the iron concentration of 20 μg $mL^{-1}$ with cell density of 1000 cells $mL^{-1}$. A specific nano-platform based on the conjugating CdTe quantum dots with $Fe_3O_4$-filled carbon nanotubes (CNTs) has been applied for in vitro simultaneous cancer-targeted optical imaging and magnetically guided drug delivery by Chen el al. [15]. The results of this work verified that $Fe_3O_4$ filled into the CNTs interior facilitates magnetically guided delivery and improves the synergetic targeting efficiency [15]. The performance of superparamagnetic iron oxide-PLGA composite microcapsules has been also evaluated for magnetic resonance-guided high-intensity focused ultrasound cancer surgery, and the observed results established the administration of PLGA-coated $Fe_3O_4$ microcapsules as potentially synergistic technique for the enhancement of MR-guided HIFU cancer surgery [19]. The superparamagnetic iron oxide carbon-based composites i.e. $Fe_3O_4$/C NPs has been also studied in the fields of adsorbent toward removal of organic dyes [21-23], removal of water pollutants from aqueous solution [24-26].

In this work, we report a novel iron oxide based composite i.e. $Ni^{2+}$ doped $Fe_3O_4$/carbon prepared through one-step simple cathodic electrodeposition (CED). It has been reported that iron oxide NPs in both form of bare and polymer coated can be easily fabricated through cathodic electrodeposition (CED) [27-31]. Furthermore, it was reported that the CED method can be applied as facile route for the doping iron oxide (i.e. $Fe_3O_4$) nanoparticles with metal ions like as $Gd^{3+}$, $Mn^{2+}$, $Dy^{3+}$, $Co^{2+}$, $La^{3+}$, $Sm^{3+}$, $Zn^{2+}$ and $Eu^{3+}$ cations [32-40]. It was reported that the carbon/magnetite composites are proper candidate for use as electrode materials for

supercapacitors and batteries [41-44]. Electrochemical synthesis provide simple, cheap, fast and safe rod for the preparation of nanomaterials, and is capable to control the crystal structure, morphology and composition of the products via proper selection of potential, current and electrolyte-type and composition [45-55]. Here, we applied cathodic electrodeposition for fabrication of $Ni^{2+}$ cations doped $Fe_3O_4$/C NPs composite. It is worth noting that the electrochemical synthesis has not been reported for the fabrication of this type of materials. The magnetic and structural properties of the prepared nan-composite are characterized by XRD, FT-IR, FE-SEM and VSM analyses. The results established that electrochemical synthesis provides facile method for fabrication of superparamagnetic composite of nickel doped iron oxide/carbon nanoparticles.

## 2. EXPERIMENTAL PROCEDURE

### 2.1. Materials

Iron(III) nitrate nonahydrate ($Fe(NO_3)_3$. $9H_2O$, 99.9%), iron(II) chloride tetrahydrate ($FeCl_2 \cdot 4H_2O$, 99%), and nickel chloride hexahydrate ($NiCl_2$ .$6H_2O$, 99.5%) were purchased from Sigma Aldrich. Carbon nanoparticles (CNPs) were received from local company. All materials were used as received and without any purification.

### 2.2. Electrochemical synthesis of composite sample

Fe(III) nitrate (2.6 g), Fe(II) chloride (0.8 g) and Ni chloride (0.5 g) were dissolved in l L deionized water. Then, 100 mg carbon nanoparticles was added into this electrolyte and sonicated for 2 h. This prepared electrolyte was used as the deposition bath in the electrochemical synthesis process. In a typical two-electrode system, the stainless-steel sheet (5 cm*10 cm) and graphite plates with same sizes were used cathode and anode electrodes, respectively. The electrochemical synthesis was performed in the constant current (CC) mode with applying 10 mA $cm^{-2}$. The deposition time and bath temperature were selected to be 30 min and 25 $^oC$, respectively. After synthesis, the deposit was scraped form the cathode electrode and washed several times with deionized water. The drying process of deposit powder was done at 80$^oC$ for 1h.

### 2.3. Sample characterization

The FTIR analysis was done at a resolution of 4 $cm^{-1}$ from 400 to 4000 $cm^{-1}$ using a Bruker Vector 22 Fourier transformed infrared spectroscope. Morphology of the prepared composite was observed using scanning electron microscopy (SEM, Mira 3-XMU with accelerating voltage of 100 kV). The crystal structure of the prepared composite was characterized via X-ray diffraction (XRD, Phillips PW-1800). The hysteresis profile and the related magnetic

properties of the prepared composite were obtained through vibrating sample magnetometer (VSM, Lake Shore Cryotronics, model 7407).

## 3. RESULTS AND DISCUSSION

Typical XRD pattern of the synthesized composite is presented in Fig. 1. All observed diffractions in this pattern are (220), (311), (400), (422), (511), (440), (620), (622) and (533), which located at 2theta of 29.2º, 34.3º, 42.5º, 55.1º, 57.6º, 63.8º and 74.9. These peaks are completely in agreement with those of iron oxide ($Fe_3O_4$) with cubic spinel structure with JCPDS number of 01-088-0315, reported in the literature [54,55], No additional peaks are observed. Also, XRD pattern do not display obvious difference compared to pristine $Fe_3O_4$ pattern reported in the literature, may be due to the amorphous structure of carbon [56]. Hence, it is verified that the Ni doped iron oxide core of the fabricated composite has magnetite crystal phase.

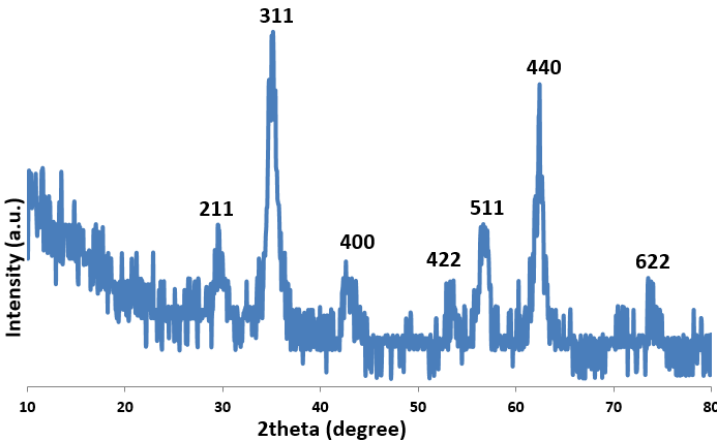


**Fig. 1.** XRD pattern of the prepared composite

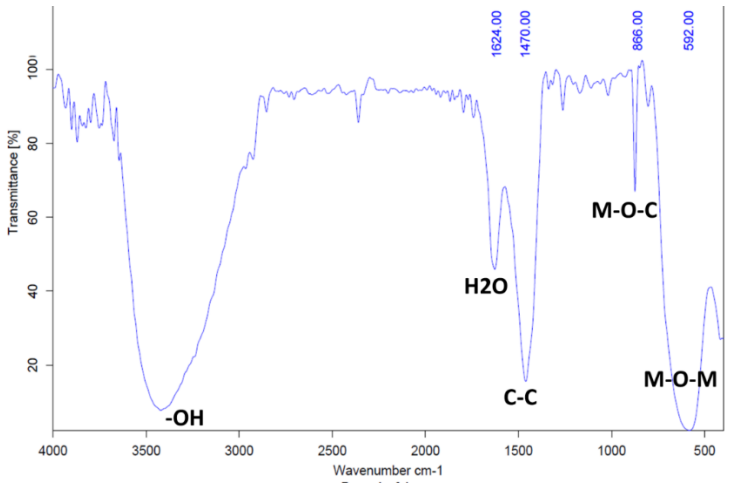


**Fig. 2.** IR spectrum of the synthesized iron oxide/carbon composite

IR spectrum of the prepared composite is shown in Fig. 3. A strong absorption peak at 586 $cm^{-1}$ corresponds to the Fe–O/Ni-O vibrations [57]. The absorption peaks at 1637 $cm^{-1}$ is related to the water molecules and OH groups attached into the magnetite NPs [58]. Also, a strong absorption bands between 3350-3500 $cm^{-1}$ were due to O–H stretching vibration [59]. Moreover, the absorption bands at 1713 $cm^{-1}$ and 1478 $cm^{-1}$ are related to the C bands [60]. A sharp IR band at 866 $cm^{-1}$ is due to the metal-oxygen-carbon stretching vibration [61]. These IR data are completely established the successful electrochemical preparation of Ni doped $Fe_3O_4$/C composite.

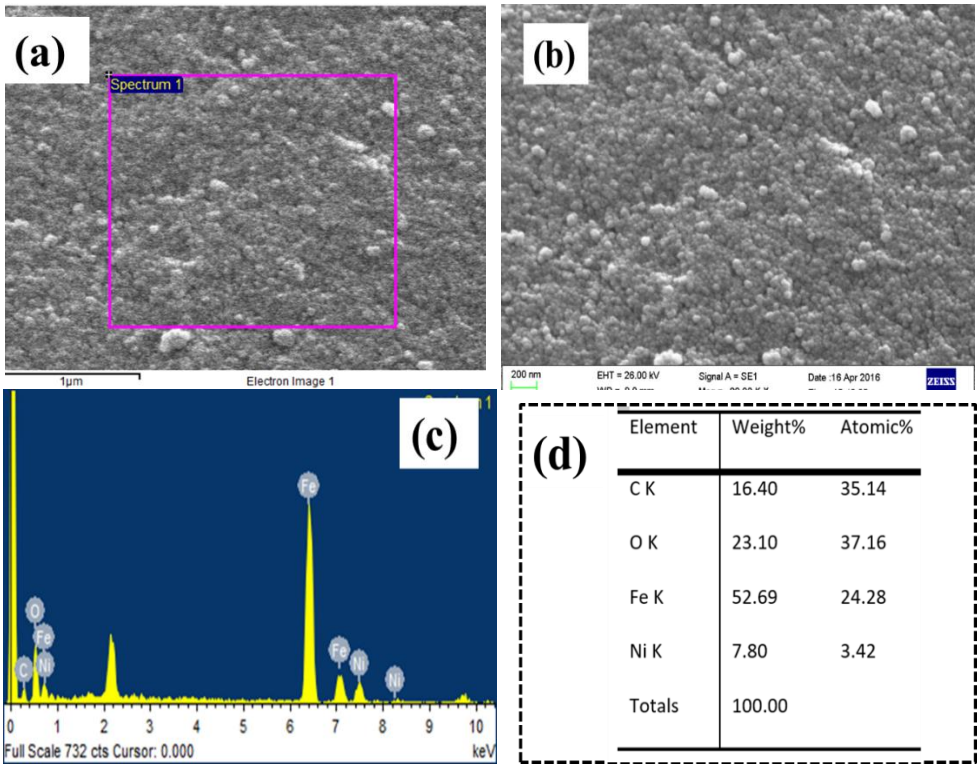


| Element | Weight% | Atomic% |
|---|---|---|
| C K | 16.40 | 35.14 |
| O K | 23.10 | 37.16 |
| Fe K | 52.69 | 24.28 |
| Ni K | 7.80 | 3.42 |
| Totals | 100.00 | |

**Fig. 3.** (a,b) FE-SEM images and (c,d) EDS data of the synthesized composite

Morphological observations via SEM and elemental analysis (EDS) data of the prepared composite are presented in Fig. 3. For the fabricated composite, well-defined uniform particle morphology are observed in the SEM images (Fig. 3a and b). The observed particles are in the range of about 20 nm. EDs graph presented in Fig. 3c indicated the presence of Fe, NI, C and O elements in the fabricated composite. The Ni doped content in the prepared composite was 7.8% (Fig. 3d), which is very close to its reported value for fabricated pristine Ni doped iron oxide at the same electrochemical conditions. In fact, it has been reported that the Ni doped magnetite prepared at the same condition applied in this work has composition of Fe (62.98 wt%), Ni (10.12 wt%) and O (26.91 wt%) [62]. The Fe and O contents of the composite sample are reduced as compared with those of pristine Ni doped $Fe_3O_4$, which is related to the

introduction of C into the Ni doped $Fe_3O_4$ structure as a surface layer. As listed in Fig. 3d, the carbon content of the composite is replacement 16.4% revealing the co-deposition of magnetite and CNPs on the cathode electrode during the applied electrochemical strategy. These data proved the fabrication of $Ni^{2+}$ doped $Fe_3O_4$/carbon composite with uniform particle morphology.

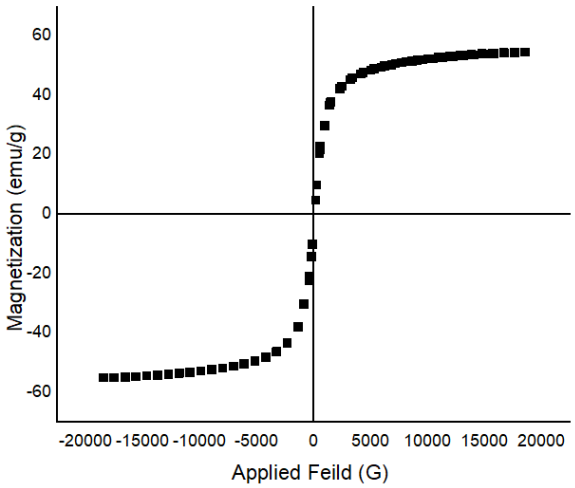


**Fig. 4.** Hysteresis profile for the prepared sample at room temperature

Magnetic properties were investigated via magnetic field dependent magnetization by applying a maximum magnetic field of ±20 kOe (1 Oe=79.59 A $m^{-1}$). Typical magnetic hysteresis loop i.e. magnetization (emu $g^{-1}$, M) *vs*. magnetizing field (Oe, H), at room temperature (298 K) is shown in Fig. 6. Magnetic properties of the fabricated composite including, saturation (Ms) and remanent (Mr) magnetizations, and coercivity field (Hci) are summarized in Table 1.

**Table 1.** Magnetic data of pristine Ni-$Fe_3O_4$ and Ni-$Fe_3O_4$/C composite

| Sample name | Ms(emu/)g | Coercively (Hci)G | Positive (Hci) G | Negative (Hci) G | Negative Mr(emu/g) | Positive Mr(emu/g) | Retentivity Mr(emu/g) | Ref. |
|---|---|---|---|---|---|---|---|---|
| Pristine Ni-$Fe_3O_4$ | 41.47 | 4.344 | 21.39 | 12.71 | -0.82 | -0.48 | 0.17 | [62] |
| Ni-$Fe_3O_4$/C composite | 54.83 | 9.26 | 7.62 | -10.9 | -0.35 | 0.51 | 0.43 | This work |

It was reported that magnetite NPs that are less than 20 nm in size, generally show superparamagnetic nature with almost zero coercivity and remenance values [60]. For our prepared composite, as there is not remanence or coercivity in the hysteresis loops of the composite, it is revealed that the composite exhibits a superparamagnetic feature [61-64]. The

*Ms*, *Mr* and *Hci* values of the composite were 54.83 emu $g^{-1}$, 0.43 emu $g^{-1}$ and 9.26 G, respectively. These data further proved the superparamagnetic nature of the prepared composite. The magnetic data of pristine N-doped $Fe_3O_4$ sample was provided from Ref. [62]. Comparing the data listed in Table 1 revealed that the composite sample exhibit higher value (Ms=54.83 emu $g^{-1}$) as respect to the pristine sample (Ms=41.47emu $g^{-1}$), may be related to the not-agglomerated morphology of composite sample (Fig. 2) and single-domain behavior of the Ni-$Fe_3O_4$/C composite electrodeposited in the presence of carbon NPs.

## 4. CONCLUSION

In summary, we introduce a simple electrochemical approach to prepare Ni doped $Fe_3O_4$/C nanocomposite. The fabricated composite exhibits uniform particle morphology with magnetite crystal structure. The Ni doped and carbon contents of the composite sample were determined to be 7.8% and 16.45, respectively. As verified by VAM data, the composite showed superparamagnetic nature, which could be suitable candidate for biomedical applications like as hyperthermia and MIR contrast agent.

## REFERENCES

[1] L. Salomão Arias, J. Pelim Pessan, A. P. Miranda Vieira, T. M. Toito de Lima, A. C. Botazzo Delbem, and D. R. Monteiro, Antibiotics 7 (2018) 46.

[2] Y. X. J. Wang, S. Xuan, M. Port, and J. M. Idee, Curr. Pharmaceut. Design 19 (2013) 6575.

[3] S. Purushotham, and R.V. Ramanujan, Acta Biomater. 6 (2010) 502.

[4] R. Kumar, A. Chauhan, S. K. Jha, and B. K. Kuanr, J. Mater. Chem. B (2018) doi:10.1039/C8TB01365A.

[5] M. Aghazadeh, and I. Karimzadeh, Curr. Nanosci. 14 (2018) 42.

[6] M. Aghazadeh, I. Karimzadeh, and M. R. Ganjali, Mater. Lett. 228 (2018)137.

[7] W. Wu, Q. He, and C. Jiang, Nanoscale Res. Lett. 3 (2008) 397.

[8] A. Ali, H. Zafar, M. Zia, I. Haq, A. R. Phull, J. S. Ali, and A. Hussain, Nanotechnol. 9 (2016) 49.

[9] M. Aghazadeh, I. Karimzadeh, M.R. Ganjali, and M. Mohebi Morad, Mater. Lett. 196 (2017) 392

[10] I. Karimzadeh, H. Rezagolipour Dizaji, and M. Aghazadeh, J. Magn. Magn. Mater. 416 (2016) 81.

[11] Y. Zhang, L. Zhang, X. Song, X. Gu, H. Sun, C. Fu, and F. Meng, J. Nanomater. (2015) 417389.

[12] W. Chen, P. Yi, Y. Zhang, L. Zhang, Z. Deng, and Z. Zhang, ACS Appl. Mater. Interfaces 3 (2011) 4085.

[13] H. S. Cho, Z. Dong, G. M. Pauletti, J. Zhang, H. Xu, H. Gu, L. Wang, R. C. Ewing, C. Huth, F. Wang, and D. Shi, ACS Nano 4 (2010) 5398.
[14] J. Carlos Ríos-Hurtado, E. M. Múzquiz-Ramos, A. Zugasti-Cruz, and D. A. Cortés-Hernández, J. Biomater. Nanobiotechnol. 7 (2016) 19.
[15] M. L. Chen, Y. J. He, X. W. Chen, and J. H. Wang, Langmuir 28 (2012) 16469.
[16] Y. X. J. Wang, D. W. Wang, X. M. Zhu, F. Zhao, K. C. F. Leung, Quant. Imaging Med. Surg. 2 (2012) 53.
[17] X. Shi, S. He Wang, S. D. Swanson, S. Ge, Z. Cao, M. E. Van Antwerp, K. J. Landmark, and J. R. Baker, Adv. Mater. 20 (2008) 1671.
[18] G. Wang, D. Zhao, N. Li, X. Wang, and Y. Ma, J. Magn. Magn. Mater. 456 (2018) 316.
[19] Y. Sun, Y. Zheng, P. Li, D. Wang, C. Niu, Y. Gong, R. Huang, Z. Wang, Z. Wang, and H. Ran, BMC Cancer 14 (2014) 800.
[20] D. Li, M. Deng, Z. Yu, Wei Liu, G. Zhou, W. Li, X. Wang, D.P. Yang, and W. Zhang, ACS Biomater. Sci. Eng. 4 (2018) 2143.
[21] M. Aghazadeh, and M. R. Ganjali, J. Mater. Sci.: Mater Electron. 28 (2017) 8144.
[22] W. Yao, C. Shen, and Y. Lu, Compos. Sci. Technol. 87 (2013) 8.
[23] R. Wu, J. H. Liu, L. Zhao, X. Zhang, J. Xie, B. Yu, X. Ma, S.T. Yang, and H. Wang, J. Environmental Chem. Engin. 2 (2014) 907.
[24] Z. Zhang, and J. Kong, J. Hazardous Mater. 193 (2011) 325.
[25] X. Bao, Z. Qiang, J.H. Chang, W. Ben, and J. Qu, J. Environmental Sci. 26 (2014) 962.
[26] Y. Zhang, S. Xu, H. Xia, and F. Zheng, Solid State Sci. 61 (2016) 16.
[27] I. Karimzadeh, M. Aghazadeh, M.R. Ganjali, and T. Dourudi, Curr. Nanosci. 13 (2017) 167.
[28] I. Karimzadeh, M. Aghazadeh, M.R. Ganjali, P. Norouzi, S. Shirvani-Arani, T. Doroudi, P. H. kolivand, S. A. Marashi, and D. Gharailou, Mater. Lett. 179 (2016) 5.
[29] M. Aghazadeh, I. Karimzadeh, and M. R. Ganjali, Mater. Lett. 209 (2017) 450.
[30] M. Aghazadeh, I. Karimzadeh, and M. R. Ganjali, J. Mater. Sci.: Mater. Electron. 28 (2017) 13532.
[31] M. Aghazadeh, I. Karimzadeh, A. Ahmadi, M. R. Ganjali and P. Norouzi, J. Mater. Sci. Mater. Electron. (2018) 14378.
[32] M. Aghazadeh, I. Karimzadeh, A. Ahmadi and M. R. Ganjali, J. Mater. Sci. Mater. Electron. (2018) 14567.
[33] H. R. Naderi, P. Norouzi and M. R. Ganjali, Applied Surface Science 366 (2016) 552.
[34] M. Aghazadeh, and M. R. Ganjali, J. Mater. Sci.: Mater. Electron. 29 (2018) 2291.
[35] M. Aghazadeh, I. Karimzadeh, M. R. Ganjali and M. G. Maragheh, J. Mater. Sci. Mater. Electron. 29 (2018) 5163.
[36] H. R. Naderi, M. R. Ganjali and A. S. Dezfuli, J. Mater. Sci. Mater. Electron. 29 (2018) 3035.

[37] M. Aghazadeh, A. Rashidi and M. R. Ganjali, Electron. Mater. Lett. 14 (2018) 37.
[38] M. Aghazadeh, I. Karimzadeh, and M. R. Ganjali, J. Electronic Mater. 47 (2018) 3026.
[39] H. R. Naderi, A. Sobhani-Nasab, M. Rahimi-Nasrabadi and M. R. Ganjali, Applied Surface Science 423 (2017) 1025.
[40] M. Aghazadeh and M. R. Ganjali, J. Mater. Sci. Mater. Electron. 28 (2017) 11406.
[41] J. Pu, L. Shen, S. Zhu, J. Wang, W. Zhang, and Z. Wang, J. Solid State Electrochem. 18 (2014) 1067
[42] M. Liu, H. Jin, E. Uchaker, Z. Xie, Y. Wang, G. Cao, S. Hou, and J. Li, Nanotechnol. 28 (2017) 155603.
[43] H. Fan, R. Niu, J. Duan, W. Liu, and W. Shen, ACS Appl. Mater. Interfaces 8 (2016) 19475.
[44] L. Zhao, M. Gao, W. Yue, Y. Jiang, Y. Wang, Y. Ren, and F. Hu, ACS Appl. Mater. Interfaces 7 (2015) 9709.
[45] J. Tizfahm, B. Safibonab, M. Aghazadeh, A. Majdabadi, and B. Sabour, Colloids Surf. A 443 (2014) 544.
[46] M. Aghazadeh, M. G. Maragheh, M. R. Ganjali, P. Norouzi and F. Faridbod, Applied Surface Science 364 (2016) 141.
[47] J. Tizfahm, M. Aghazadeh, M. G. Maragheh, M. R. Ganjali, P. Norouzi and F. Faridbod, Mater. Lett. 167 (2016) 153.
[48] M. Aghazadeh, M. Asadi, M. R. Ganjali, P. Norouzi, B. Sabour and M. Emamalizadeh, Thin Solid Films 634 (2017) 24.
[49] M. Aghazadeh, A. A. M. Barmi, H. M. Shiri, and S. Sedaghat, Ceram. Int. 39 (2013) 1045.
[50] M. Aghazadeh, M. Asadi, M. G. Maragheh, M. R. Ganjali, P. Norouzi and F. Faridbod, Applied Surface Science 364 (2016) 726.
[51] M. Aghazadeh, R. Ahmadi, D. Gharailou, M. R. Ganjali, and P. Norouzi, J. Mater. Sci. Mater. Electron. 27 (2016) 8623.
[52] I. Karimzadeh, M. Aghazadeh, M. R. Ganjali, P. Norouzi, T. Doroudi and P. H. Kolivand, Mater. Lett. 189 (2017) 290.
[53] M. Aghazadeh, M. R. Ganjali, and P. Norouzi, J. Mater. Sci.: Mater. Electron. 27 (2016) 7707.
[54] K. S. Loh, Y. H. Lee, A. Musa, A. A. Salmah, and I. Zamri, Sensors 8 (2008) 5775.
[55] P. Arévalo, J. Isasi, A. C. Caballero, J. F. Marco, and F. Martín-Hernández, Ceram. Int. 43 (2017) 10333.
[56] Q. Wu, M. Chen, K. Chen, S. Wang, C. Wang, and G. Diao, J. Mater. Sci. 51 (2016) 1572.
[57] M. Aghazadeh, Mater. Lett. 211 (2018) 225.

[58] M. Aghazadeh, A. Bahrami-Samani, D. Gharailou, M. Ghannadi Maragheh, and M. R. Ganjali, J. Mater. Sci.: Mater. Electron. 27 (2016) 11192.
[59] Y. Wei, B. Han, X. Hu, Y. Lin, X. Wang, and X. Deng, Procedia Engin. 27 (2012) 632.
[60] X. Yang, W. Chen, J. Huang, Y. Zhou, Y. Zhu, and C. Li, Sci. Rep. 5 (2015) 10632.
[61] J. Moradiganjeh, and Z. Aghajani, J. Mater. Sci.: Mater. Electron. 27 (2016) 5948.
[62] M. Aghazadeh, and M. R. Ganjali, J. Mater. Sci.: Mater. Electron. 29 (2018) 4981.
[63] N. Sinan, and E. Unur, Mater. Chem. Phys. 183 (2016) 571.
[64] C. Zou, Y. Yao, N. Wei, Y. Gong, W. Fu, M. Wang, L. Jiang, X. Liao, G. Yin, Z. Huang, and X. Chen, Composites Part B 77 (2015) 209.